

# Earth's Future

## RESEARCH ARTICLE

10.1029/2018EF001047

### Key Points:

- Methodological choices can have large impacts on projected changes in hydrology, at times affecting the sign of change in streamflow volume
- Changes in flow timing are mostly explained by modeled changes in climate while changes in low flows by hydrologic model choice
- The spread among our projected changes remains large, but it is possible to focus modeling efforts to better understand the spread

### Supporting Information:

- Supporting Information S1

### Correspondence to:

B. Nijssen,  
nijssen@uw.edu

### Citation:

Chegwidden, O. S., Nijssen, B., Rupp, D. E., Arnold, J. R., Clark, M. P., Hamman, J. J., et al. (2019). How do modeling decisions affect the spread among hydrologic climate change projections? Exploring a large ensemble of simulations across a diversity of hydroclimates. *Earth's Future*, 7, 623–637. <https://doi.org/10.1029/2018EF001047>

Received 14 SEP 2018

Accepted 26 APR 2019

Accepted article online 30 APR 2019

Published online 17 JUN 2019

©2019. The Authors.

This is an open access article under the terms of the Creative Commons Attribution-NonCommercial-NoDerivs License, which permits use and distribution in any medium, provided the original work is properly cited, the use is non-commercial and no modifications or adaptations are made.

## How Do Modeling Decisions Affect the Spread Among Hydrologic Climate Change Projections? Exploring a Large Ensemble of Simulations Across a Diversity of Hydroclimates

Oriana S. Chegwidden<sup>1</sup> , Bart Nijssen<sup>1</sup> , David E. Rupp<sup>2</sup> , Jeffrey R. Arnold<sup>3</sup> , Martyn P. Clark<sup>4,5</sup> , Joseph J. Hamman<sup>4,6</sup> , Shih-Chieh Kao<sup>7</sup> , Yixin Mao<sup>1</sup> , Naoki Mizukami<sup>4</sup> , Philip W. Mote<sup>2</sup> , Ming Pan<sup>8</sup> , Erik Pytlak<sup>9</sup> , and Mu Xiao<sup>10</sup> 

<sup>1</sup>Civil and Environmental Engineering, University of Washington, Seattle, WA, USA, <sup>2</sup>Oregon Climate Change Research Institute, Oregon State University, Corvallis, OR, USA, <sup>3</sup>United States Army Corps of Engineers, Climate Preparedness and Resilience Program, Seattle, WA, USA, <sup>4</sup>Research Applications Laboratory, National Center for Atmospheric Research, Boulder, CO, USA, <sup>5</sup>Now at Coldwater Laboratory, University of Saskatchewan, Canmore, Alberta, Canada, <sup>6</sup>Now at Climate and Global Dynamics, National Center for Atmospheric Research, Boulder, CO, USA, <sup>7</sup>Environmental Sciences Division, Oak Ridge National Laboratory, Oak Ridge, TN, USA, <sup>8</sup>Civil and Environmental Engineering, Princeton University, Princeton, NJ, USA, <sup>9</sup>Bonneville Power Administration, Portland, OR, USA, <sup>10</sup>Geography, University of California, Los Angeles, CA, USA

**Abstract** Methodological choices can have strong effects on projections of climate change impacts on hydrology. In this study, we investigate the ways in which four different steps in the modeling chain influence the spread in projected changes of different aspects of hydrology. To form the basis of these analyses, we constructed an ensemble of 160 simulations from permutations of two Representative Concentration Pathways, 10 global climate models, two downscaling methods, and four hydrologic model implementations. The study is situated in the Pacific Northwest of North America, which has relevance to a diverse, multinational cast of stakeholders. We analyze the effects of each modeling decision on changes in gridded hydrologic variables of snow water equivalent and runoff, as well as streamflow at point locations. Results show that the choice of representative concentration pathway or global climate model is the driving contributor to the spread in annual streamflow volume and timing. On the other hand, hydrologic model implementation explains most of the spread in changes in low flows. Finally, by grouping the results by climate region the results have the potential to be generalized beyond the Pacific Northwest. Future hydrologic impact assessments can use these results to better tailor their modeling efforts.

**Plain Language Summary** Future climate change will affect water resources throughout the Pacific Northwest of North America. Simulation experiments and recent observations agree that there will be less snow and it will melt earlier, which will impact the timing and amount of streamflow. However, the magnitudes of these changes are uncertain. In this study, we analyzed the spread among 160 different simulated scenarios of the hydrologic future. We show that the ways we represent the future atmosphere and land surface can have strong effects on our final predictions. Specifically, the way that we model the land surface has a large impact on predictions in arid zones or during dry periods. However, the way we model the atmosphere affects our predictions of changes in snow, snowmelt, and streamflow timing. Our findings are helpful for understanding future hydrologic change more thoroughly, which is of particular importance given international agreements in the Columbia River Basin.

## 1. Introduction

Robust analysis of hydrologic climate change requires an understanding of the spread among the projections of the estimated impacts. To quantify and assess this spread, the field of hydrologic projection has moved away from single simulation or small ensemble studies of future traces. Instead, it is increasingly popular to create large ensembles representing an array of possible hydrologic futures (Addor et al., 2014; Bosshard et al., 2013; Dobler et al., 2012; Finger et al., 2012; Harding et al., 2012; Hattermann et al., 2018; Lafaysse et al., 2014; Mendoza et al., 2015; Mizukami et al., 2016; Prudhomme & Davies, 2009; Vidal et al., 2016; Wilby & Harris, 2006). The string of models used to create these ensembles has been termed

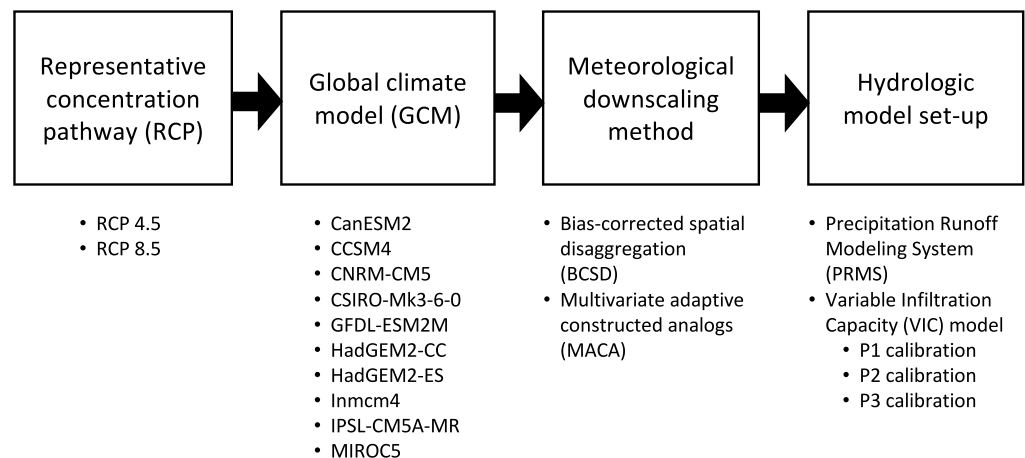


**Figure 1.** The study described in this paper consisted of four model decision points represented by the boxes above. Every permutation of the bulleted list of modeling options was evaluated to create the study's ensemble.

the *impact modeling chain* (Bosshard et al., 2013). These chains consist of a series of sequential modeling steps that ingest climate information and produce estimates of hydrologic impacts. An example of one such chain (the one implemented for this paper) is shown in Figure 1. Each step in the chain requires the selection of a model from a variety of modeling options. By implementing multiple options for every modeling decision, we can investigate the ways in which modeling decisions affect our projections.

The use of ensemble approaches to assess the impact of model choice is well established. Hawkins and Sutton (2009, 2011) attributed uncertainty in regional temperature and precipitation projections to choices of global climate model (GCM), representative concentration pathway (RCP), and internal variability (IV). The choice of hydrologic model implementation has been shown to have a strong influence within the hydrologic modeling impact chain in a variety of smaller basin studies (Addor et al., 2014; Jung et al., 2012; Najafi et al., 2011; Wilby & Harris, 2006), though Chen et al. (2011) found relatively smaller influences of hydrologic model choice compared to the choice of GCM. Hattermann et al. (2018) investigated the relative contributions of steps of the impact modeling chain on changes in streamflow across nine river basins across the globe. They found that the largest determinants of spread in changes in mean and high streamflow volumes are GCM and RCP, but that changes in low flows were more likely driven by hydrologic model choice. However, their analyses did not extend to the effect of hydrologic model parameterization and did not account for IV. Addor et al. (2014) noted the potential benefits of conducting an uncertainty analysis across many diverse basins or a larger domain but acknowledged the computational challenges of an analysis of that scale. In summary, while comprehensive studies are common within smaller basins, it is difficult to obtain large-scale experiments that allow for consistent comparisons across modeling decisions.

In this paper, we conduct an experiment across a large and hydroclimatically diverse region: the Pacific Northwest of North America (PNW, Figure 2). We analyze an ensemble of future hydrologic scenarios using multiple options for four modeling decisions (see Figure 1). By combining every option from each decision in a factorial experiment we created 160 different possible hydrologic futures for the region (Chegwidden et al., 2017). We also explicitly account for the role of IV or the natural fluctuations of the Earth system that deviate from an externally forced long-term trend. Lafaysse et al. (2014) and Alder and Hostetler (2019) emphasize the importance of this line of analysis, though it has otherwise often been neglected in hydrologic impacts studies.

Anthropogenic climate change and its hydrological impacts in the PNW have been extensively studied (Elsner et al., 2010; Schnorbus et al., 2014; Werner et al., 2013). Abatzoglou et al. (2014) have noted that anthropogenic climate change has already caused statistically significant increases in temperature during the second part of the twentieth century across the PNW. The changes, and their associated observed impacts on hydrology (Casola et al., 2009; Hidalgo et al., 2009; Mote et al., 2005, 2018; Stoelinga et al., 2010), are projected to continue during the 21st century (Rupp et al., 2017).

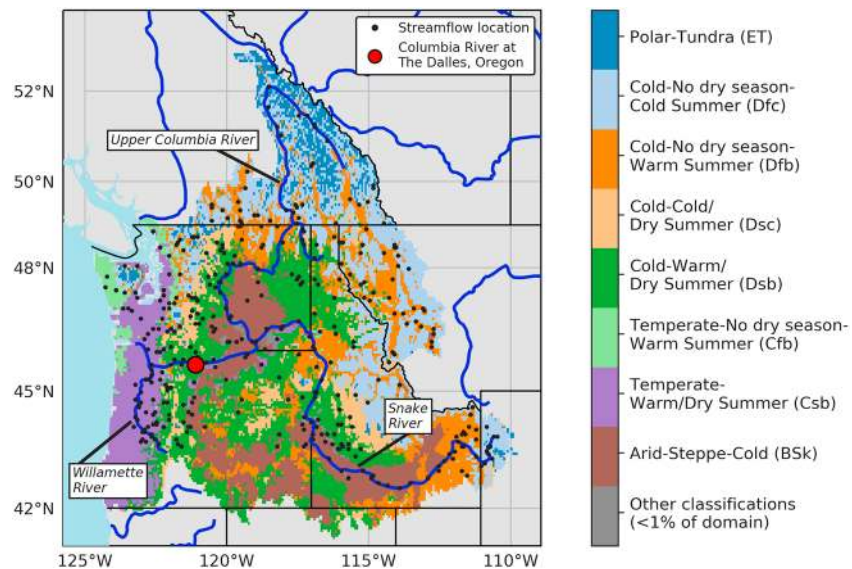


**Figure 2.** The study domain classified by Köppen-Geiger climatic regime. Streamflow locations are shown as black dots.

In this paper, we specifically use the term *spread* as opposed to *uncertainty* to emphasize that our ensemble is a subsample of the true distribution of all possible future scenarios. As a result, our numerical results are specific to our ensemble. Nevertheless, by incorporating multiple modeling options and conducting our analyses across a hydroclimatically diverse domain, we aim for our spread to capture much of that uncertainty space and thus make our findings more generally applicable.

Understanding the spread among projected changes is of critical interest given the extensive management of the Columbia River. These infrastructure projects are used for flood risk management, hydropower generation, irrigation water needs, recreation, and navigation. The dams also impact fish and ecosystem services, with notable relevance to First Nations. Further, because the basin straddles the border between the United States and Canada, the projected streamflow impacts have particular political significance. The two nations signed the Columbia River Treaty in 1964 outlining how the river would be managed and operated economically (U.S Army Corps of Engineers, 2012). In 2013 the Columbia River Management Joint Operating Committee called for research to investigate climate change impacts for the Columbia River through the end of the 21st century, in part to inform the ongoing regional and international management of the river for the 21st century. Our study responds to these interests, with particular emphasis on the spread among the projected changes.

This paper answers two main questions:

1. How does model spread depend on choice of evaluation metric and location? The diversity of climatic regimes and 150-year temporal extent of our study aid in answering this question.
2. What effect do our modeling choices have on projections of hydrologic change? The factorial construction of this ensemble allows us to draw robust conclusions about the contribution of methodological choices to the spread among projections.

## 2. Methods

### 2.1. Study Domain

We conducted our study over the Columbia River Basin (drainage area 668,000 km<sup>2</sup>) in the PNW as well as the United States (US) coastal Pacific Ocean drainages (Figure 2). The PNW is characterized by contrasting climatic regimes. The western slopes of the Cascade and Olympic Mountains in the Pacific coastal drainages experience moderate temperatures and receive some of the highest precipitation in North America, more than 6,000 mm annually (see the left panels of Figures S1 and 3). Conversely, some

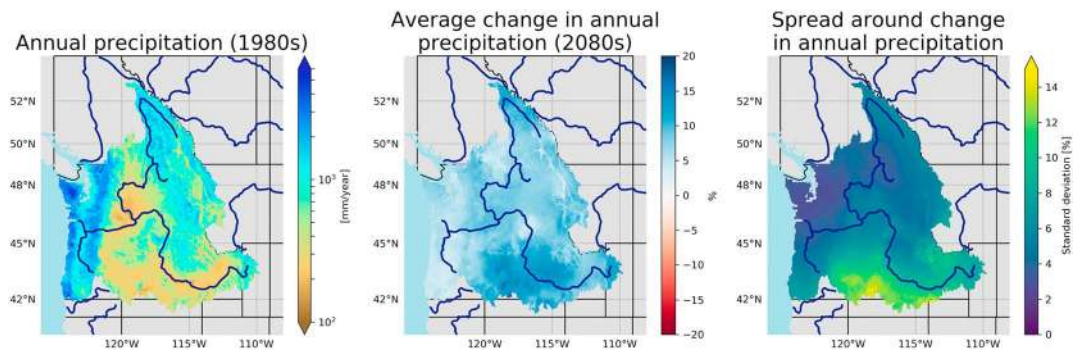


**Figure 3.** Historical mean annual precipitation (left), changes by the 2080s (center), and the spread around those changes (right) according to all 10 GCMs for RCP 8.5. GCMs = global climate models; RCP = Representative Concentration Pathway.

locations in the interior of the Columbia Basin receive an average of less than 100 mm annually. The Columbia Basin is bounded to the east and north by the cold, moist Rocky Mountains. Historically, precipitation within the mountainous regions has been winter dominant, causing the region's hydrology to be snowmelt driven.

## 2.2. Historical Data Sets

A gridded meteorological forcing data set (1/16th degree, ~6 km; Livneh et al., 2013) encompassing the PNW domain was used as a basis for meteorological bias correction and two of the four hydrologic model calibrations. Reference streamflow data were taken from the *no regulation, no irrigation* (NRNI) streamflow data set (River Management Joint Operating Committee, 2017), which provides time series at 190 sites throughout the PNW for the water years (WY) 1928–2008 (a water year in the western United States is the period from 1 October in the previous year through 30 September of the current year). The NRNI data set removes the effects of regulation, irrigation, and reservoir evaporation from measured streamflow and can be used as a proxy for naturalized streamflow to support hydrologic model calibration.

## 2.3. Methodological Choices

### 2.3.1. Representative Concentration Pathways

We selected climate simulations from the repository compiled by the Coupled Model Intercomparison Project Phase 5 (Taylor et al., 2012). For this study, we used the RCPs corresponding to a high emissions scenario (RCP 8.5) and a midrange mitigation emissions scenario (RCP 4.5) as described in Taylor et al. (2012). As in Addor et al. (2014) we chose to include the RCP as another modeling choice to investigate how global changes affect local hydrology.

### 2.3.2. Global Climate Models

We selected ten GCMs (Figure 1) for this study by ranking each model's ability to best reproduce a variety of observed metrics over the historical period within the PNW (Rupp et al., 2013). We further based our GCM selection on their ability to represent mesoscale atmospheric dynamics, which we assessed by evaluating 500-hPa heights in the control simulations.

### 2.3.3. Meteorological Forcing Downscaling Methods

Two statistical meteorological forcing downscaling method (DSM) techniques were used to downscale each of the 20 RCP/GCM combinations to the 1/16th degree (~6 km) grid resolution. The bias correction, spatial disaggregation (BCSD, Wood et al., 2004) method was implemented at the monthly time step. The multivariate adaptive constructed analogs (MACA) approach was implemented at the daily time step as described in Abatzoglou and Brown (2012). The Livneh et al. (2013) data set from 1950 to 2005 was used as the reference for the bias-correction step of the DSMs. The resulting statistically downscaled GCM data include control simulations (1950–2005) and climate change projections (2006–2099).

### 2.3.4. Hydrologic Model Implementations

The downscaled Coupled Model Intercomparison Project Phase 5 meteorology was used to force four distinct hydrologic model implementations (Table 1). All hydrologic modeling was conducted on the same 1/16th degree grid with results available at a daily time step from 1950 to 2099. Two different hydrologic model codes were used in this project: the Variable Infiltration Capacity (VIC; Liang et al., 1994) model

**Table 1**  
Descriptions of the Four Hydrologic Models (Columns) Referenced in the Rightmost Column of Figure 1

	VIC-P1	PRMS-P1	VIC-P2	VIC-P3
Calibrated parameters	$b_1$ , depth of soil layers 2 and 3, Ksat, Nijssen (2001) parameters D1, D2, D3	slowcoef_sq, sat_threshold, pref_flow_den, gwflow_coef, ssr2gw_rate, snowinfil_max, soil2gw_max, soil_moist_max	See Oubeidillah et al. (2014)	See Mizukami et al. (2017)
Calibration methodology	Inverse calibration	Inverse calibration	Lumped basin calibration	Calibrated parameter transfer functions
Reference meteorological data set	Livneh et al. (2013)	Livneh et al. (2013)	Daymet (Thornton et al., 1997)	Livneh et al. (2013)
Reference streamflow data set	No-regulation, no-irrigation flows (RMJOC, 2017)	No-regulation, no-irrigation flows (RMJOC, 2017)	USGS WaterWatch gauges at monthly time step (Brakebill et al., 2011)	Hydro-Climate Data Network basins (Newman et al., 2014)

Note. USGS = United States Geological Survey.

and the Precipitation Runoff Modeling System (PRMS; Leavesley et al., 1983). Both are process-based, energy balance models. The VIC model code included a newly developed glacier model (Hamman & Nijssen, 2015) uses a volume-area scaling relationship (Bahr et al., 1997) to estimate the areal coverage of a glacier within a grid cell. When the areal coverage of the glacier exceeds the area allocated to a given elevation zone, the model moves ice to lower, warmer elevation zones enabling glacier melt. We used three unique VIC implementations, each with independently derived parameter sets, denoted as P1, P2, and P3. Each VIC simulation was initialized with a 255-year spin-up run to allow for sufficient initialization of the glacier model. The PRMS simulations involved a 20-year spin-up. Within this paper, *hydrologic model* (HM) will refer to the combination of model code and parameter set. Historical performance of the four HMs is displayed in Figure S2.

The VIC-P1 and PRMS-P1 implementations (Table 1) were developed specifically for this study. For both implementations, we calibrated model parameters in the Columbia Basin upstream of Bonneville Dam and the Willamette River Basin. We selected the NRNI streamflow time series at 60 sites to create a spatially distributed set of runoff time series using the approach detailed in Pan and Wood (2013). Each grid cell in the VIC-P1 and PRMS-P1 HMs was then calibrated independently in a method we call "inverse calibration" in Table 1. We implemented the shuffled complex evolution calibration method (Duan et al., 1993) maximizing the weekly Kling-Gupta Efficiency (KGE) statistic for WY 1992–2001 (Gupta et al., 2009). For coastal drainages we used parameters from a previous Columbia River climate change study (Hamlet et al., 2013) for VIC-P1. We developed the noncalibrated soil parameters for the PRMS-P1 implementation by merging the State Soil Geographic Database for the United States portion of the domain and the Canadian Soil Survey (Soil Classification Working Group, 1998) and followed methods recommended in the PRMS documentation to develop PRMS parameters (United States Geological Survey, 2009).

The VIC-P2 implementation used the same vegetation parameter sets as those used in VIC-P1, but with soil and snow band parameters as described by Oubeidillah et al. (2014). The simulated runoff at each HUC8 subbasin was calibrated to United States Geological Survey WaterWatch runoff at the monthly time step using the Daymet meteorological forcing data set (Brakebill et al., 2011; Thornton et al., 1997), in contrast to the other three setups which used Livneh et al. (2013). Parameters were used as-is except for the area upstream of Hungry Horse Dam which was calibrated to NRNI for that gage to improve model performance for that subbasin.

The VIC-P3 implementation used the same vegetation and snow band parameters as VIC-P1, but with a soil parameter set developed using the multiscale parameter regionalization method (Mizukami et al., 2017). Instead of the traditional parameter calibration, this technique calibrates the parameters of transfer functions that relate soil and landscape properties to model parameters for a subset of a domain. The transfer functions can then be used domain wide to estimate model parameters outside of the calibration basins. Transfer function parameters were calibrated at a daily time step for unimpaired or Hydro-Climate Data Network basins and applied to the continental United States to produce spatially consistent parameters for the entire domain (Newman et al., 2014).

#### 2.4. Streamflow Routing

Modeled runoff fields were routed to 396 sites throughout the domain (see streamflow locations in Figure 2; Chegwidden et al., 2017) using the RVIC routing model (Hamman et al., 2017), a source-to-sink model based on the Lohmann et al. (1996) routing model. The same routing setup was used for all simulations. It does not account for any water management (e.g., reservoirs or withdrawals), and the resulting streamflows (and our ensuing analyses) do not address uncertainties related to water management modeling or operations.

#### 2.5. Analysis of Variance

We focused our analyses on spreads in projected changes in streamflow and assessed how model decisions and IV contribute to those spreads. We compared streamflow for a 30-year control period (the 1980s, consisting of WY 1970–1999) with a 30-year future period (2080s, WY 2070–2099). For each of these periods, we calculated three streamflow metrics: (1) centroid of timing, defined as the day of the water year when 50% of the annual flow volume has passed a streamflow location, (2) annual volume, and (3) annual minimum 7-day flow. We calculated the change signal for each ensemble member separately and thus created a 160-member ensemble of projected change signals from the 1980s to the 2080s. We examined the change signals as opposed to the future values themselves to control for systematic differences in the model setups.

We used this ensemble of projected changes in streamflow to evaluate the impact of methodological choices on those projected changes. We developed a methodology inspired by previous uncertainty analysis studies (e.g., Alder & Hostetler, 2019; Bosshard et al., 2013; Hawkins & Sutton, 2009), but we highlight that our methods (1) focus on changes in 30-year means and (2) explicitly account for IV.

To estimate IV, we assumed that each metric responds linearly to the radiative forcing in a given RCP. Specifically, for each annual time series (1950–2099) of each metric and streamflow location, we fitted a linear model  $x = af + b$ , where  $x$  is the predicted annual values of the metric,  $f$  is the annual values of radiative forcing corresponding to the respective RCP, and  $a$  and  $b$  are the fitted coefficients. We used the residuals  $\epsilon$  of the fit to estimate the IV of a change in 30-year mean. See section S2 in the supporting information for a detailed description.

We used analysis of variance (ANOVA) to assess the impacts of methodological choices on the spread of the projections of change in the 30-year means from the fitted time series  $x(t)$ . Our final variance analyses can be summarized as

$$TV = IV + MV \quad (1)$$

where TV is the total variability in a change projection, IV is the internal variability of the projected change, and MV is the model variability defined as

$$MV = RCP + GCM + DSM + HM + GCM : RCP + HM : GCM + Residual \quad (2)$$

where RCP, GCM, DSM, and HM are the portions of variance explained by the corresponding methodological choices. (Note that the *Residual* in equation (2) is distinct from residual  $\epsilon$  used to estimate IV.) The interaction terms  $GCM : RCP$  and  $HM : GCM$  were the dominant terms in the residual error in the variance. We lumped other interaction terms into the residual term in equation (2) to preserve degrees of freedom within the ANOVA analysis.

#### 2.6. Climate Classifications

We applied ANOVA at every model grid cell in the domain. The grid cells were grouped according to the updated Köppen-Geiger classification scheme (Peel et al., 2007) based on the monthly temperature and precipitation data from Livneh et al. (2013) for the historical period 1970–1999. Over 99% of grid cells were classified into eight climate regions (Figure 2). The remaining <1% of the grid cells were excluded from the analyses for simplicity.

### 3. Hydrologic Impacts of Climate Change and Projection Spread

Snow accumulation and melt are the dominant drivers of the hydrologic cycle in the Columbia River basin. As temperature increases and snow presence decreases, the role of snow storage will diminish. In this

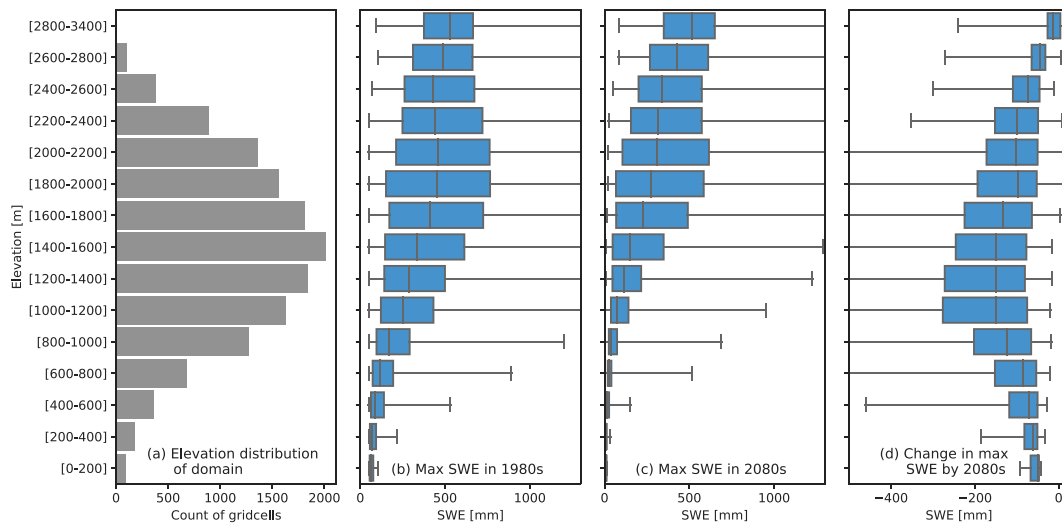


**Figure 4.** For fifteen elevation zones shown in (a), the distribution of modeled snow water equivalent (SWE) for the 1980s (b), the 2080s using RCP 8.5 (c), and the difference (d). In the last three panels, boxes and whiskers indicate minimum, median, and maximum values and the interquartile range.

section, we briefly review the dominant climate change impacts on the hydrology of the Columbia River Basin but focus our analysis on the spread within the ensemble of projections. The projected changes in hydrologic variables are in overall agreement with previous work in the PNW (Elsner et al., 2010; Hamlet et al., 2013).

### 3.1. Changes in Snowpack in the PNW

For our snow analyses we only considered areas where snow accumulation and melt are an important hydrologic process, which we defined as grid cells with more than 50 mm of annual maximum snow water equivalent (SWE) during the historical period. The elevation profile of these areas is shown in Figure 4a. The areas between 1,000 and 1,800 m are projected to experience the highest losses of maximum SWE, with median decreases of 150 mm by the 2080s (RCP 8.5). The spread in the changes is largest for elevations between 1,000 and 1,400 m (Figure 4d). The spreads are narrower at the lowest and highest elevations because little snow is present at low elevations and winter temperatures remain below freezing at high elevations despite anthropogenic warming.

The median date of annual maximum peak SWE for the 1980s as simulated within the ensemble is shown in Figure 5a, and the median change in the date of peak SWE is shown in Figure 5b (RCP 8.5). While annual maxima of peak SWE occurred historically in March, for much of the domain, the date of peak SWE is projected to occur approximately 20 to 40 days earlier by the 2080s. The standard deviation of the projected changes in peak SWE date is shown in Figure 5c and can be interpreted as a measure of the ensemble spread. The greatest spread in change in peak SWE date occurs on the western side of the Cascades and the Olympic mountains. These areas lie in the transient snow zone and already experience significant midwinter melt episodes during the historic period.

### 3.2. Annual Streamflow Changes and Model Agreement

Annual streamflow volumes are projected to increase at all locations in the domain. This is consistent with a general increase in precipitation across the PNW (Figure 3). Changes in seasonal streamflow between the control and future periods are shown in the left panel of Figure 6 for winter (December-January-February), spring (March-April-May), summer (June-July-August), and autumn (September-October-November). Streamflow is projected to increase at all locations in winter and spring. Summer streamflow is, on average, projected to decrease owing predominantly to an earlier shift in snowmelt onset accompanied by a reduction in summer precipitation and increases in evaporation due to higher temperatures. Changes in streamflow across the basin are further discussed in River Management Joint Operating Committee (2018).

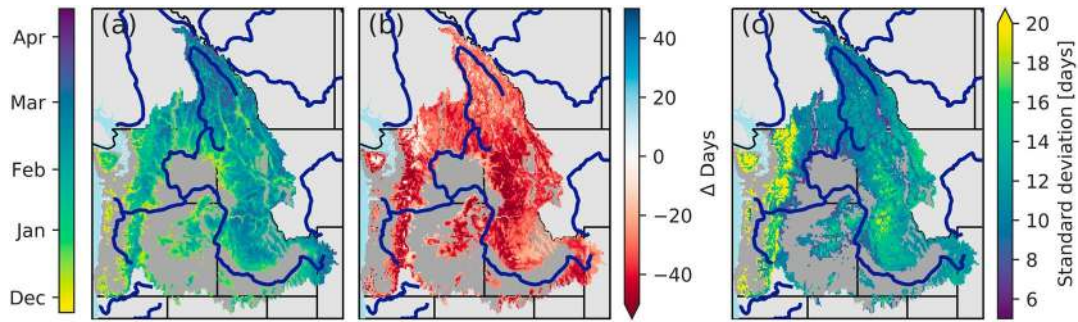


**Figure 5.** The date of median annual maximum SWE for the 1980s is shown in Figure 5a. The ensemble (RCP 8.5) median change in the date of peak SWE by the 2080s is shown in Figure 5b. The standard deviation (measure of spread) of the distribution of projected changes in date of peak SWE is shown in Figure 5c.

We analyzed the ensemble to determine the level of agreement regarding streamflow increases or decreases between the control and future periods (four right panels in Figure 6). Ensemble agreement has been shown to be a good summary indicator of overall ensemble behavior (Melsen et al., 2017). Green colors indicate that the ensemble generally agrees that streamflow will increase, while purple colors indicate agreement on a decrease. Lighter colors indicate disagreement among the ensemble members.

Models agree that streamflow will increase at almost all locations in winter and decrease at almost all locations in summer. Models agree that spring streamflow will increase for most locations as a result of the earlier shift of the snowmelt peak. Model agreement is smallest during autumn. The most notable disagreement is along the Snake River in the southeast of the study domain in the autumn where 110 ensemble members project increases and 50 project decreases. While percentage changes in streamflow are smallest in autumn, late summer/early autumn is also a critical period for many locations so small streamflow changes could still significantly impact water users.

#### 4. Contribution of Methodological Choices to Ensemble Spread

In this section, we will evaluate the spread within the ensemble projections of hydrologic change in different regions and determine how methodological choices impact the spread.

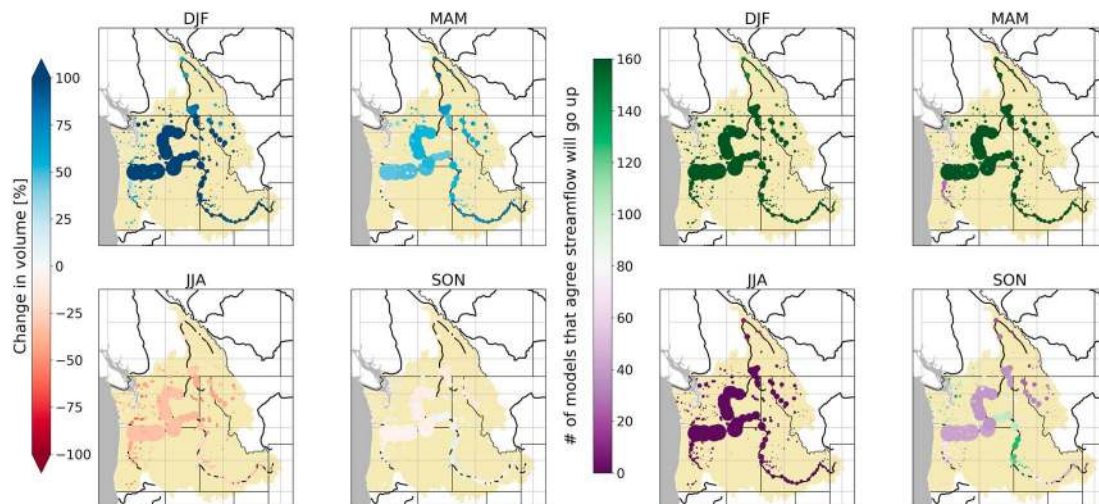


**Figure 6.** Changes (from control to future periods) in mean seasonal streamflow volumes for locations throughout the domain for winter (DJF), spring (MAM), summer (JJA), and autumn (SON) are shown in the left panel. The right panel shows the model agreement on the direction of streamflow change. Streamflow location marker sizes are scaled by the mean annual historic NRNI flow. DJF = December-January-February; MAM = March-April-May; SON = September-October-November; JJA = June-July-August.



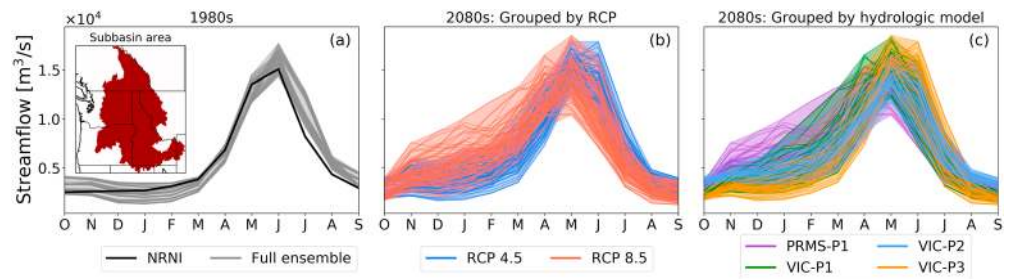


**Figure 7.** Ensemble seasonal hydrographs for the Columbia River at The Dalles. The basin area is highlighted in red in the inset map. Each trace represents a different ensemble member. (a) The historical 1980s climatological period including the no-regulation, no-irrigation reference flow in black. (b and c) The projected streamflow by the 2080s, grouped, respectively, by RCP choice and HM choice.

#### 4.1. Streamflow Seasonality for the Columbia River Basin

Mean monthly hydrographs for the 160-member ensemble for the Columbia River at The Dalles (red marker in Figure 2) are shown in Figure 7. Every line in the spaghetti plot represents a single ensemble member for a given 30-year period. The gray traces in Figure 5a represent the 1980s climatological period. Within the historic period the streamflows lie close to the NRNI reference flow (shown in black), indicating good skill of the modeling setup in reproducing the historic reference flow.

The traces in Figures 7b and 7c are identical but are highlighted differently to show the effect that methodological choice has on streamflow projections. In Figure 7b, the ensemble is grouped by emissions scenario. In Figure 7c, the ensemble is grouped by HM. By the 2080s, the RCP 4.5 simulations show the snowmelt-related streamflow peak in either May or June whereas RCP 8.5 simulations peak a month earlier. Furthermore, the RCP 8.5 simulations show large increases in winter streamflow. By the 2080s, the spread in simulations widens, particularly in the winter months when shifts from snow to rain regimes differ among the models.

Comparing groupings in Figure 7c, PRMS-P1 simulations show the greatest sensitivity to the changed climate of the 2080s, as they exhibit the greatest increases in winter streamflow. VIC-P1 and VIC-P3 simulations exhibit shifts in the peak toward April and May, but VIC-P2 shows the least sensitivity to the changing climate.

#### 4.2. Impact of Modeling Decisions on Ensemble's Distribution of Centroid Shift

The shift in centroid of timing is an indicator of overall changes in streamflow timing. The full ensemble's distribution of changes in the centroid of timing (from control to future periods) for the Columbia River at The Dalles is shown in Figure 8. The Gaussian kernel density estimate (KDE) of the full ensemble is shown in the black line in every panel of Figure 8. The projected timing shifts range from zero to 60 days earlier. The KDE of timing shifts is decomposed according to three different methodological choices: RCP (Figure 8a), GCM (Figure 8b), and HM (Figure 8c). The effect of DSM choice is not shown as the distinction between BCSD and MACA had minimal impact on the timing shift for this location. Choice of RCP has a large impact on the timing shift at The Dalles, with a mean timing shift of 19 days earlier for RCP 4.5 and 35 days earlier for RCP 8.5. The timing shifts grouped by GCM are also markedly distinct, with differences between some GCMs as large as between RCPs. PRMS-P1 was associated with the largest changes in centroid of timing while simulations from VIC-P2 showed the smallest shift.

#### 4.3. Contribution of Each Modeling Component to Ensemble Spread

The ANOVA quantifies the contribution of each modeling choice to the spread in changes. The pie charts in Figure 9 show, for 12 representative locations throughout the domain, how much each modeling choice, as well as IV, explains changes in different metrics: centroid of timing (Figure 9a), annual volume (Figure 9b), and low flows (Figure 9c). The size of each pie is proportional to the total variance in that metric at that location. Overall, choice of RCP drives the spread in the change in timing, choice of GCM contributes most toward the spread in the change in volume, and choice of HM explains most of the spread in change in the magnitude of the low flows.

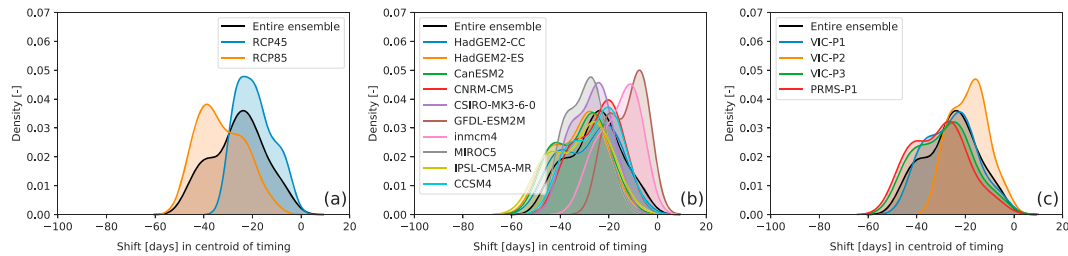


**Figure 8.** Distribution of the full ensemble's projected changes (1980s to 2080s) in centroid of timing for streamflow of the Columbia River at The Dalles, Oregon. The black line represents the full ensemble of projected changes and is identical in all three panels. In each panel the distribution is decomposed into simulations sourced from different methodological options. The distribution is separated according to (a) RCP choice, (b) GCM choice, and (c) HM choice.

Figure 10 highlights the dominant driver of the spread in the change for all metrics at all locations in the domain. For downstream locations, RCP tends to be the dominant contributor to the spread in timing shift (Figure 10a). The choice of GCM is the dominant contributor to the spread among locations in the Upper Columbia, the Willamette, and small coastal drainages in Washington State.

Changes in annual volume (Figures 9b and 10b) are largely controlled by the choice of GCM, given annual volume's dependence on precipitation. The control of GCM on volume change is strongest along the Snake River where GCMs show a large spread in precipitation changes (Figure 2). In contrast, when the spread of projected precipitation change is small, as along the mainstem of the Columbia above the confluence with the Snake River, HM choice is most relevant to explaining the spread.

The spread in changes in low flows (Figures 9c and 10c) are largely explained by choice of HM. The low flow period in the domain occurs typically in the drier early autumn when snow and soil moisture stores are depleted. Because changes in low flows are driven by soil processes as opposed to precipitation, and each HM had distinct soil parameter data sets (VIC implementations) or different process representation (VIC versus PRMS), the baseflow from each model varies widely. The exception to this relationship appears in the Snake where the diversity among precipitation projections overrides low flow generation so that changes in low flows are controlled more by GCM than HM.

#### 4.4. Generalizing Results by Climatic Region

We conducted the ANOVA for the runoff from every grid cell in the domain and averaged the results across each of the eight climate regions (Figure 11). The averaging gives every grid cell equal weight, regardless of its contribution to the streamflow of the basin. In this way, we see how each region responds but do not

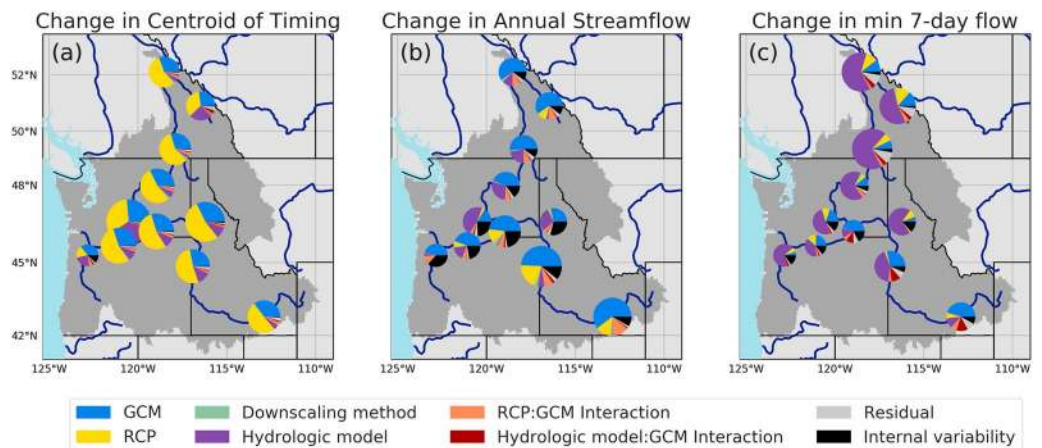


**Figure 9.** ANOVA results for the change in three metrics between the 1980s and the 2080s. The portion of variance of the change explained by each methodological choice is shown for selected sites of interest. The size of each marker is scaled by the standard deviation of the ensemble for that metric and location.

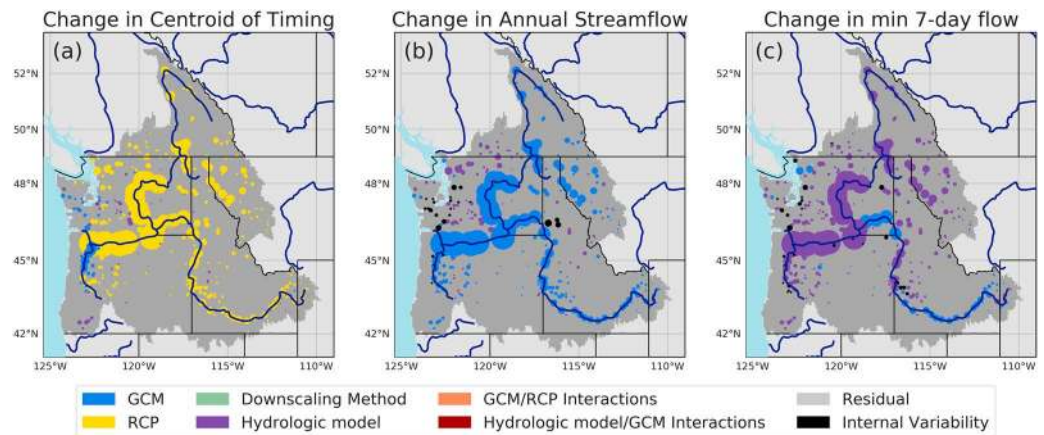


**Figure 10.** The dominant contributor to the variance of the projected changes in three metrics from the 1980s to the 2080s: (a) change in centroid of timing, (b) change in annual streamflow, and (c) change in low flows. Marker sizes are scaled by the mean annual historic NRNI flow.

expect the results to agree with those conducted at streamflow locations that aggregate across upstream area, thus emphasizing grid cells with greater runoff contributions. We leverage the diversity of the domain to elucidate general patterns linking hydroclimatic regime, metric of interest, and model spread to inform future hydroclimate impacts studies.

**4.4.1. RCP Choice Impactful for Timing in Areas Susceptible to Large Changes in Snowpack**

As seen in Figure 11a, midelevation cold areas (Dfc) comprise the region affected most by RCP choice for the change in timing. The Dfc region is also projected to experience significantly larger losses in snowpack according to RCP 8.5 as compared to RCP 4.5 (Figure 3), meaning that the choice of RCP would have a pronounced impact on the resulting changes for these regions. The same relationship does not apply to the lower elevation Dfb regions which are expected to lose nearly all of their snowpack by the 2080s, making the choice of RCP less important for those regions (Figure 11a).

**4.4.2. Choice of HM More Important in Water-Limited Regimes**

When evaporative and baseflow processes account for a larger portion of the water balance (whether in low flow periods or in arid locations), the choice of HM becomes a more impactful decision, in agreement with Vidal et al. (2016). The dominance of HM in the change in low flows seen in Figures 9c and 10c is again evident across climatic regime (Figure 11c). Choice of HM was the dominant driver of the change in centroid of timing for arid sections of the domain (Figure 11a). Across all climatic regimes, GCM-HM interactions contributed more to the spread in the low flow metric than to the other two metrics.

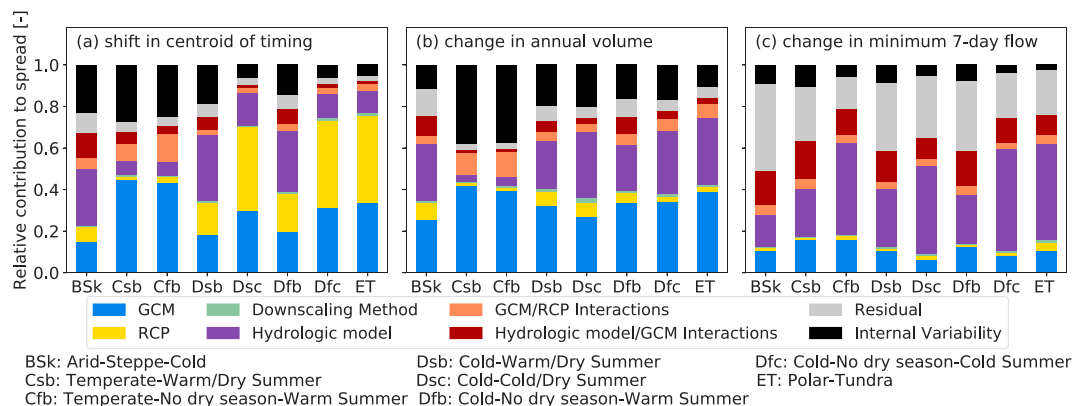


**Figure 11.** The ANOVA results grouped by climatic regime are shown above. The relative size of each color band denotes how much each methodological choice explains the spread in the change in each region.

#### 4.4.3. GCM Choice and IV More Important for Energy-Limited Regimes

The majority of the streamflow in the PNW originates in energy-limited environments, as seen by the overlap of the high-precipitation areas in Figure 3 and the cold, wet regions (Dfc, Dfb) in Figure 2. In these regions, changes in precipitation are strongly correlated with changes in annual streamflow volumes. Choice of GCM is a much larger contributor to change in precipitation than is RCP. Thus, the choice of GCM is the dominant contributor to spread in annual volume, as confirmed by Figure 10b.

The impact of GCM choice is enhanced when the GCMs lack consensus about the projected changes in precipitation, which aligns with findings from Melsen et al. (2017). For example, in the Willamette River Basin, precipitation is projected to increase between 2% and 5%, but with a standard deviation of about 5% (Figure 2). Thus, some GCMs project increases in precipitation and others decreases. This same region is the basin with the most disagreement on the direction of change in annual streamflow (Figure S3). Accordingly, the choice of GCM accounted for about 50% of the total spread in projections for the Willamette River Basin, with IV and GCM-RCP interactions accounting for nearly the entire remainder.

IV is more important (and sometimes becomes the dominant contributor to the spread) when precipitation changes are the most significant driver. For example, across the three metrics, IV is most important for changes in annual streamflow. Further, IV is more important for the temperate coastal regions in the domain (Csb and Cfb in Figure 11), even for changes in centroid of timing, where rain- (as opposed to snow-) dominance results in a strong dependence of centroid of timing on changes in precipitation rather than temperature. The IV contribution is smaller for our results than those reported by Alder and Hostetler (2019), who used a shorter 11-year averaging window instead of our 30-year averaging window.

#### 4.4.4. Changes in Annual Streamflow Explained Most by GCM Selection

Figures 9b and 10b show that the choice of GCM along with its interaction with RCP accounts for the largest portion of the spread in projections of change in annual volume for this ensemble. This is particularly true in the temperate regions of the domain (Csb and Cfb) where choice of HM has negligible impact. In these regions, the runoff ratio is so high that, with precipitation as the main driver, GCM and its interaction with RCP account for nearly the entire spread in the projected changes.

#### 4.4.5. Choice of DSM Did Not Explain Spread for the Regions and Metrics Studied

The difference between the two statistical DSMs (BCSD and MACA) was not an important contributor to the spread in this study's metrics or domains. Choice of DSM contributed most to the spread in projections of changes in annual volume in the arid, smaller basins of the domain, in agreement with Jiang et al. (2018). However, this paper does not address extreme high flows where the two statistical DSMs are expected to differ more substantially in their projections of precipitation changes given that the two techniques were implemented at different time steps: BCSD at monthly and MACA at daily. Nevertheless, our ensemble did use the same meteorological data set for training both DSMs and, as Alder and Hostetler (2019) note, the training data set can have a strong influence on projected changes in snowpack. We acknowledge that DSM choice might have contributed more to ensemble spread had our modeling chain included additional DSMs (e.g., other statistical techniques or dynamical downscaling). This is supported by the work of Gutmann et al. (2014) who evaluated differences among a large number of statistical downscaling methods and established particularly strong impacts on precipitation estimates.

#### 4.4.6. Residual Most Relevant in Water-Limited Situations

The spread is most explained by the residual when water is limited, either by climate (i.e., arid regions) or by our analysis focusing on low flows. For example, in Figure 11c we see that the residual is one of the strongest contributors to low flows at the grid cell level. In some of the smaller arid basins of the southeastern domain the residuals even become the dominant contributor to the spread (Figure 10c).

## 5. Conclusions

Our findings about hydrologic changes in the PNW in response to climate change are generally consistent with other studies (Elsner et al., 2010; Hamlet et al., 2013). However, the spread among the projections is considerably wider as a result of expanding the number of modeling options used to create the ensemble. While the ensemble projects decreasing peak SWE throughout the domain, the spread among those projections is widest in midelevation areas where changes are projected to be greatest. Further, the ensemble is in good agreement that Canadian portions of the basin are likely to retain a large part of their snowpack

through the end of the 21st century. This shift in snow retention has significant implications for international agreements regarding water resources planning. The ensemble agrees overwhelmingly that winter streamflows will increase across the domain. There is also overwhelming agreement that summertime streamflows will decrease. Most disagreement exists in projections of autumn streamflow, especially in smaller tributaries. The disagreement in these locations highlights that there is generally less consistency among projections of climate change impacts on smaller upstream areas.

Our analyses offer guidance for future hydrologic climate impacts studies. The extent to which each modeling decision contributes to the spread in projections of change depends on both location and metric of interest. Choice of RCP is most impactful when changes in snowmelt will affect the region or metric. For situations in which the GCMs disagree about changes in precipitation, and in particular in energy-limited environments, GCM selection is most important. Choice of HM is a larger contributor for situations in which soil processes are more active (e.g., low flows and arid environments). The dominance of the residual in water-limited situations necessitates further work to evaluate how modeling components interact. This is of particular interest given the acute stresses that these low-flow periods have upon water users and ecosystems.

Our findings are largely robust to the IV in the system. Overall, the role of IV is strongest when precipitation is a driving factor, moderate when temperature is the driving factor, and smallest when the HM is the driving factor. Nevertheless, for the 30-year period over which we calculated our metrics, model variance exceeds that of IV. Thus, modeling choices have a greater impact on our results than the natural variability in the system. As Hawkins and Sutton (2009) note, the portion of variance contributed by IV is irreducible since it comes from the natural climate system. On the other hand, the model variance highlights areas where model refinement could improve hydrologic projections of climate change impacts.

These findings can inform future modeling efforts by leading to a select set of recommendations. While increasing the number of ensemble end-members improves the understanding of the spread in projections, based on our results it may be possible to tailor a future study to the questions of interest. One could emphasize analysis and resources within the model decision step that accounts for the most spread in the ensemble for any metric of interest. For example, for adequately understanding climate change impacts on low flows, it may be an efficient use of resources to evaluate how and why hydrologic models differ in their sensitivities of changes in low flows. Within this domain and this ensemble, the influence of DSM choice was negligible compared to that of GCM choice, but we only investigated two statistical DSMs and thus likely underestimate DSM contribution to model spread. Therefore, it may be useful to shift efforts toward incorporating more GCMs into an ensemble, particularly in areas with high runoff ratios where changes in precipitation will be the driving factor determining metrics like changes in annual volume.

To best aid water resources preparedness, it is critical that modeling efforts capture the most representative range of possible outcomes. Given perennial computational constraints, we might derive more confidence in future projections by emphasizing model diversity at steps in the chain most relevant for our research questions.

#### Acknowledgments

This work was funded in part by the Bonneville Power Administration's Technology and Innovation Program under grant TIP 304 to the University of Washington and Oregon State University. Additional support was provided by the United States Army Corps of Engineers Climate Preparedness and Resilience Programs and the Bureau of Reclamation under Cooperative Agreement R17AC00024 to the University of Washington. The authors thank Eric Salathé at the University of Washington who assisted in implementing the BCSD system. The MACA-downscaled data were provided by John Abatzoglou and Katherine Hegewisch at the University of Idaho. We also thank Lieke Melsen and an anonymous reviewer for their insightful comments on this manuscript. The data set described in this paper is available via Chegwidden et al. (2017). The VIC model is available at <https://github.com/UW-Hydro/VIC/releases/tag/VIC.4.2.glacier.01>. The PRMS model is available at [https://www.brr.cr.usgs.gov/projects/SW\\_MoWS/PRMS.html](https://www.brr.cr.usgs.gov/projects/SW_MoWS/PRMS.html).

#### References

- Abatzoglou, J. T., & Brown, T. J. (2012). A comparison of statistical downscaling methods suited for wildfire applications. *International Journal of Climatology*, 32(5), 772–780. <https://doi.org/10.1002/joc.2312>
- Abatzoglou, J. T., Rupp, D. E., & Mote, P. W. (2014). Seasonal climate variability and change in the Pacific Northwest of the United States. *Journal of Climate*, 27(5), 2125–2142. <https://doi.org/10.1175/JCLI-D-13-00218.1>
- Addor, N., Rössler, O., Köplin, N., Huss, M., Weingartner, R., & Seibert, J. (2014). Robust changes and sources of uncertainty in the projected hydrological regimes of Swiss catchments. *Water Resources Research*, 50, 7541–7562. <https://doi.org/10.1002/2014WR015549>
- Alder, J. R., & Hostetler, S. W. (2019). The dependence of hydroclimate projections in snow-dominated regions of the western United States on the choice of statistically downscaled climate data. *Water Resources Research*, 55, 2279–2300. <https://doi.org/10.1029/2018WR023458>
- Bahr, D. B., Meier, M. F., & Peckham, S. D. (1997). The physical basis of glacier volume-area scaling. *Journal of Geophysical Research*, 102(B9), 20,355–20,362. <https://doi.org/10.1029/97JB01696>
- Bosshard, T., Carambia, M., Goergen, K., Kotlarski, S., Krahe, P., Zappa, M., & Schär, C. (2013). Quantifying uncertainty sources in an ensemble of hydrological climate-impact projections. *Water Resources Research*, 49, 1523–1536. <https://doi.org/10.1029/2011WR011533>
- Brakebill, J. W., Wolock, D. M., & Terziotti, S. E. (2011). Digital hydrologic networks supporting applications related to spatially referenced regression modeling. *Journal of the American Water Resources Association*, 47(5), 916–932. <https://doi.org/10.1111/j.1752-1688.2011.00578.x>
- Casola, J. H., Cuo, L., Livneh, B., Lettenmaier, D. P., Stoelinga, M. T., Mote, P. W., & Wallace, J. M. (2009). Assessing the impacts of global warming on snowpack in the Washington cascades. *Journal of Climate*, 22(10), 2758–2772. <https://doi.org/10.1175/2008JCLI2612.1>

- Chegwidden, O. S., Nijssen, B., Rupp, D. E., & Mote, P. W. (2017). Hydrologic response of the Columbia River System to climate change [Data set]. Zenodo. Retrieved from doi:<https://doi.org/10.5281/zenodo.854763>
- Chen, J., Brissette, F. P., Poulin, A., & Leconte, R. (2011). Overall uncertainty study of the hydrological impacts of climate change for a Canadian watershed. *Water Resources Research*, *47*, W12509. <https://doi.org/10.1029/2011WR010602>
- Dobler, C., Hagemann, S., Wilby, R. L., & StÄtter, J. (2012). Quantifying different sources of uncertainty in hydrological projections in an Alpine watershed. *Hydrology and Earth System Sciences*, *16*(11), 4343–4360. <https://doi.org/10.5194/hess-16-4343-2012>
- Duan, Q. Y., Gupta, V. K., & Sorooshian, S. (1993). Shuffled complex evolution approach for effective and efficient global minimization. *Journal of Optimization Theory and Applications*, *76*(3), 501–521. <https://doi.org/10.1007/BF00939380>
- Elsner, M. M., Cuo, L., Voisin, N., Deems, J. S., Hamlet, A. F., Vano, J. A., et al. (2010). Implications of 21st century climate change for the hydrology of Washington State. *Climatic Change*, *102*(1–2), 225–260. <https://doi.org/10.1007/s10584-010-9855-0>
- Finger, D., Heinrich, G., Gobiet, A., & Bauder, A. (2012). Projections of future water resources and their uncertainty in a glaciated catchment in the Swiss Alps and the subsequent effects on hydropower production during the 21st century. *Water Resources Research*, *48*, W02521. <https://doi.org/10.1029/2011WR010733>
- Gupta, H. V., Kling, H., Yilmaz, K. K., & Martinez, G. F. (2009). Decomposition of the mean squared error and NSE performance criteria: Implications for improving hydrological modelling. *Journal of Hydrology*, *377*(1–2), 80–91. <https://doi.org/10.1016/j.jhydrol.2009.08.003>
- Gutmann, E., Pruiitt, T., Clark, M. P., Brekke, L., Arnold, J. R., Raff, D. A., & Rasmussen, R. M. (2014). An intercomparison of statistical downscaling methods used for water resource assessments in the United States. *Water Resources Research*, *50*, 7167–7186. <https://doi.org/10.1002/2014WR015559>
- Hamlet, A. F., Elsner, M. M., Mauger, G. S., Lee, S.-Y., Tohver, I., & Norheim, R. A. (2013). An overview of the Columbia basin climate change scenarios project: Approach, methods, and summary of key results. *Atmosphere-Ocean*, *51*(4), 392–415. <https://doi.org/10.1080/07055900.2013.819555>
- Hamman, J., & Nijssen, B. (2015). VIC 4.2.glaclier. Retrieved from <https://github.com/UW-Hydro/VIC/tree/support/VIC.4.2.glaclier>
- Hamman, J., Nijssen, B., Roberts, A., Craig, A., Maslowski, W., & Osinski, R. (2017). The coastal streamflow flux in the Regional Arctic System Model. *Journal of Geophysical Research: Oceans*, *122*, 1683–1701. <https://doi.org/10.1002/2016JC012323>
- Harding, B. L., Wood, A. W., Prairie, J. R., & Service, N. W. (2012). The implications of climate change scenario selection for future streamflow projection in the Upper Colorado River basin. *Hydrology and Earth System Sciences*, *16*, 3989–4007. <https://doi.org/10.5194/hess-16-3989-2012>
- Hattermann, F. F., Vetter, T., Breuer, L., Su, B., Daggupati, P., Donnelly, C., et al. (2018). Sources of uncertainty in hydrological climate impact assessment: A cross-scale study. *Environmental Research Letters*, *13*(1), 15006. <https://doi.org/10.1088/1748-9326/aa9938>
- Hawkins, E., & Sutton, R. (2009). The potential to narrow uncertainty in regional climate predictions. *Bulletin of the American Meteorological Society*, *90*(8), 1095–1107. <https://doi.org/10.1175/2009BAMS2607.1>
- Hawkins, E., & Sutton, R. (2011). The potential to narrow uncertainty in projections of regional precipitation change. *Climate Dynamics*, *37*(1), 407–418. <https://doi.org/10.1007/s00382-010-0810-6>
- Hidalgo, H. G., Das, T., Dettinger, M. D., Cayan, D. R., Pierce, D. W., Barnett, T. P., et al. (2009). Detection and attribution of streamflow timing changes to climate change in the western United States. *Journal of Climate*, *22*(13), 3838–3855. <https://doi.org/10.1175/2009JCLI2470.1>
- Jiang, Y., Kim, J. B., Still, C. J., Kerns, B. K., Kline, J. D., & Cunningham, P. G. (2018). Inter-comparison of multiple statistically downscaled climate datasets for the Pacific Northwest, USA. *Scientific Data*, *5*, 180016. <https://doi.org/10.1038/sdata.2018.16>
- Jung, I. W., Moradkhani, H., & Chang, H. (2012). Uncertainty assessment of climate change impacts for hydrologically distinct river basins. *Journal of Hydrology*, *466–467*, 73–87. <https://doi.org/10.1016/j.jhydrol.2012.08.002>
- Lafaysse, M., Hingray, B., Mezghani, A., Gailhard, J., & Terray, L. (2014). Internal variability and model uncertainty components. *Water Resources Research*, *50*, 3317–3341. <https://doi.org/10.1002/2013WR014897>
- Leavesley, G. H., Lichty, R. W., Troutman, B. M., & Saindon, L. G. (1983). Precipitation-runoff modeling system—User's manual. U.S. Geological Survey Water-Resources Investigations Report, 83(4238), 207.
- Liang, X., Lettenmaier, D. P., Wood, E. F., & Burges, S. J. (1994). A simple hydrologically based model of land surface water and energy fluxes for general circulation models. *Journal of Geophysical Research*, *99*(D7), 14,415–14,428. <https://doi.org/10.1029/94JD00483>
- Livneh, B., Rosenberg, E. A., Lin, C., Nijssen, B., Mishra, V., Andreadis, K. M., et al. (2013). A long-term hydrologically based dataset of land surface fluxes and states for the conterminous United States: Update and extensions. *Journal of Climate*, *26*(23), 9384–9392. <https://doi.org/10.1175/JCLI-D-12-00508.1>
- Lohmann, D., Nolte-Holube, R., & Raschke, E. (1996). A large-scale horizontal routing model to be coupled to land surface parametrization schemes. *Tellus Series A: Dynamic Meteorology and Oceanography*, *48*(5), 708–721. <https://doi.org/10.3402/tellusa.v48i5.12200>
- Melsen, L., Addor, N., Mizukami, N., Newman, A., Torfs, P., Clark, M., et al. (2017). Mapping (dis)agreement in hydrologic projections. *Hydrology and Earth System Sciences Discussions*, 1–35. <https://doi.org/10.5194/hess-2017-564>
- Mendoza, P. A., Clark, M. P., Mizukami, N., Newman, A. J., Barlage, M., Gutmann, E. D., et al. (2015). Effects of hydrologic model choice and calibration on the portrayal of climate change impacts. *Journal of Hydrometeorology*, *16*(2), 762–780. <https://doi.org/10.1175/JHM-D-14-0104.1>
- Mizukami, N., Clark, M. P., Gutmann, E. D., Mendoza, P. A., Newman, A. J., Nijssen, B., et al. (2016). Implications of the Methodological choices for hydrologic portrayals of climate change over the contiguous United States: Statistically downscaled forcing data and hydrologic models. *Journal of Hydrometeorology*, *17*(1), 73–98. <https://doi.org/10.1175/JHM-D-14-0187.1>
- Mizukami, N., Clark, M. P., Newman, A. J., Wood, A. W., Gutmann, E. D., Nijssen, B., et al. (2017). Towards seamless large-domain parameter estimation for hydrologic models. *Water Resources Research*, *53*, 8020–8040. <https://doi.org/10.1002/2017WR020401>
- Mote, P. W., Hamlet, A. F., Clark, M. P., & Lettenmaier, D. P. (2005). Declining mountain snowpack in western north America. *Bulletin of the American Meteorological Society*, *86*(1), 39–49. <https://doi.org/10.1175/BAMS-86-1-39>
- Mote, P. W., Li, S., Lettenmaier, D. P., Xiao, M., & Engel, R. (2018). Dramatic declines in snowpack in the western US. *Npj Climate and Atmospheric Science*, *1*(1), 2. <https://doi.org/10.1038/s41612-018-0012-1>
- Najafi, M. R., Moradkhani, H., & Jung, I. W. (2011). Assessing the uncertainties of hydrologic model selection in climate change impact studies. *Hydrological Processes*, *25*(18), 2814–2826. <https://doi.org/10.1002/hyp.8043>
- Newman, A., Sampson, K., Clark, M. P., Bock, A. R., Viger, R. J., & Blodgett, D. L. (2014). *A Large-Sample Watershed-Scale Hydro-meteorological Dataset for the Contiguous USA*. Boulder, CO: UCAR/NCAR. <https://doi.org/10.5065/D6MW2F4D>
- Oubeidillah, A. A., Kao, S. C., Ashfaq, M., Naz, B. S., & Tootle, G. (2014). A large-scale, high-resolution hydrological model parameter data set for climate change impact assessment for the conterminous US. *Hydrology and Earth System Sciences*, *18*(1), 67–84. <https://doi.org/10.5194/hess-18-67-2014>

- Pan, M., & Wood, E. F. (2013). Inverse streamflow routing. *Hydrology and Earth System Sciences*, 17(11), 4577–4588. <https://doi.org/10.5194/hess-17-4577-2013>
- Peel, M. C., Finlayson, B. L., & McMahon, T. A. (2007). Updated world map of the Köppen-Geiger climate classification. *Hydrology and Earth System Sciences*, 11(5), 1633–1644. <https://doi.org/10.5194/hess-11-1633-2007>
- Prudhomme, C., & Davies, H. (2009). Assessing uncertainties in climate change impact analyses on the river flow regimes in the UK. Part 2: Future climate. *Climatic Change*, 93(1–2), 197–222. <https://doi.org/10.1007/s10584-008-9461-6>
- River Management Joint Operating Committee (2017). NRNI flows 1929–2008 corrected 04-2017. Bonneville Power Administration. Retrieved from <https://www.bpa.gov/p/Power-Products/Historical-Streamflow-Data/Pages/No-Regulation-No-Irrigation-Data.aspx>
- River Management Joint Operating Committee (2018). Climate and hydrology datasets for RMJOC long-term planning studies, second edition: Part 1—Hydroclimate projections and analyses. Retrieved from <https://www.bpa.gov/p/Generation/Hydro/Pages/Climate-Change-FCRPS-Hydro.aspx>
- Rupp, D. E., Abatzoglou, J. T., Hegewisch, K. C., & Mote, P. W. (2013). Evaluation of CMIP5 20th century climate simulations for the Pacific Northwest USA. *Journal of Geophysical Research: Atmospheres*, 118, 10,884–10,906. <https://doi.org/10.1002/jgrd.50843>
- Rupp, D. E., Abatzoglou, J. T., & Mote, P. W. (2017). Projections of 21st century climate of the Columbia River basin. *Climate Dynamics*, 49(5–6), 1783–1799. <https://doi.org/10.1007/s00382-016-3418-7>
- Schnorbus, M., Werner, A., & Bennett, K. (2014). Impacts of climate change in three hydrologic regimes in British Columbia, Canada. *Hydrological Processes*, 28(3), 1170–1189. <https://doi.org/10.1002/hyp.9661>
- Soil Classification Working Group. (1998). The Canadian system of soil classification.
- Stoelinga, M. T., Albright, M. D., & Mass, C. F. (2010). A new look at snowpack trends in the Cascade Mountains. *Journal of Climate*, 23(10), 2473–2491. <https://doi.org/10.1175/2009JCLI2911.1>
- Taylor, K. E., Stouffer, R. J., & Meehl, G. A. (2012). An overview of CMIP5 and the experiment design. *Bulletin of the American Meteorological Society*, 93(4), 485–498. <https://doi.org/10.1175/BAMS-D-11-00094.1>
- Thornton, P. E., Running, S. W., & White, M. A. (1997). Generating surfaces of daily meteorological variables over large regions of complex terrain. *Journal of Hydrology*, 190(3–4), 214–251. [https://doi.org/10.1016/S0022-1694\(96\)03128-9](https://doi.org/10.1016/S0022-1694(96)03128-9)
- U.S. Army Corps of Engineers (2012). Columbia River treaty history and treaty review.
- United States Geological Survey (2009). Modeling of watershed systems GSFLOW training class material: Instructions for GSFLOW model input preparation.
- Vidal, J. P., Hingray, B., Magand, C., Sauquet, E., & Ducharme, A. (2016). Hierarchy of climate and hydrological uncertainties in transient low-flow projections. *Hydrology and Earth System Sciences*, 20(9), 3651–3672. <https://doi.org/10.5194/hess-20-3651-2016>
- Werner, A. T., Schnorbus, M. A., Shrestha, R. R., & Eckstrand, H. D. (2013). Spatial and temporal change in the hydro-climatology of the Canadian portion of the Columbia river basin under multiple emissions scenarios. *Atmosphere-Ocean*, 51(4), 357–379. <https://doi.org/10.1080/07055900.2013.821400>
- Wilby, R. L., & Harris, I. (2006). A framework for assessing uncertainties in climate change impacts: Low-flow scenarios for the River Thames, UK. *Water Resources Research*, 42, W02419. <https://doi.org/10.1029/2005WR004065>
- Wood, A. W., Leung, L. R., Sridhar, V., & Lettenmaier, D. P. (2004). Hydrologic implications of dynamical and statistical approaches to downscaling climate model outputs. *Climatic Change*, 62(1–3), 189–216. <https://doi.org/10.1023/B:CLIM.0000013685.99609.9e>